



10 FEBRUARI 2021

SHOREFACE RESPONSE OF THE HOLLAND COAST TO SEA- LEVEL RISE

MASTER'S THESIS

ELINE VAN HEERWAARDEN

EARTH, SURFACE & WATER, FACULTY OF GEOSCIENCES, UTRECHT UNIVERSITY
Supervisors: Dr. T.D.Price & Dr.ir. J.H.Nienhuis



Table of Contents

1. Abstract	2
2. Introduction.....	3
3. Background	3
3.1 General coastal response.....	3
3.2 History of the Holland coast	4
3.3 Holland coast response to sea-level rise	6
3.4 Modelled sea-level rise	6
3.5 Depth of closure	7
3.6 Shoreface response rate.....	9
3.8 Research question	10
4. Methods	10
4.1 JARKUS data.....	10
4.2 Depth of closure	12
4.3 Shoreface response rates	13
5. Results.....	13
5.1 Depth of closure.....	13
5.2 Depth of closure trends	14
5.3 Shoreface response rate.....	17
6. Discussion	18
6.1 Spatial variability	18
6.2 Time evolution	18
6.3 Shoreface response rate.....	19
7. Conclusions	20
8. References	21

1. Abstract

Sea-level rise in coastal zones is a great threat to the people living there. Therefore, it is very crucial that the morphodynamic response of a coast to sea-level rise is understood. Model studies have shown that the response is a retreat of the shoreline. However, many of these studies use a contested method called the Bruun Rule (Bruun, 1983). The Holland coast offers an interesting case study for shoreface response, as there are several decades worth of yearly bathymetry measurements (JARKUS). Using a selection of the data from this dataset, the spatial and temporal variability of the depth of closure was determined as well as a shoreface response rate for the Holland coast. The depth of closure was determined from the standard deviation over time for every profile. With a moving time window, a timeseries in depth of closure was obtained. The shoreface response rate was determined using a volumetric differences approach. Depth of closure was found to have a large spatial variability, with the mean for the Holland coast being approximately 12 meters below mean sea level. The temporal variability in depth of closure is smaller than the spatial, with no clear trend or pattern emerging. A closer look at a single profile shows that nourishments can completely determine the temporal evolution of the depth of closure. Shoreface response rates are found in the order of magnitude of $1 \cdot 10^3 - 1 \cdot 10^4 \text{ m}^3\text{m}^{-1}\text{year}^{-1}$. These values remain very uncertain and further research is advised. Overall, the Holland coast is completely dominated by the human interference. For natural responses to sea-level rise an area with less human interference should be investigated.

2. Introduction

Sea-level rise is an important issue for many coastal areas as the morphodynamic response of coasts is unknown. With large parts of the world's population living in coastal areas, accurate predictions are essential. As a coastal area that has a long history of human interference and monitoring, the Holland coast is an interesting area to look at.

The objective of this study is to consider the effect of sea-level rise on the sediment balance of the Holland coast, with a specific focus on the shoreface fluxes.

3. Background

3.1 General coastal response

It is generally understood that the immediate response of low coastal areas to sea-level rise is flooding. An expected longer-term effect is coastal erosion. The impacts on a coast will be a combination of climate induced sea-level rise and local processes that can influence relative sea-level rise like glacial uplift. (Nicholls & Cazenave, 2010)

A shoreface is shaped by the balance between the wave energy and the sediment availability, within the controls of its geological inheritance (Kinsela et al., 2020). It has been established that for concave profiles the wave energy results in an onshore transport of sediment, while there is an aeolian loss term and a loss term from sea-level rise. With sea-level rise rates growing the loss term from sea-level rise will become dominant, leading to a retreat of the shoreline. (Stive, 2004)

Vousdoukas et al. (2020) predicted the shoreline response of sandy coasts around the globe, the results of which can be seen in figure 1. However, their methods are contested by Cooper et al. (2020), who argue that the method used does not accurately capture the variability in responses possible. They mention landwards retreat, erosion and even progradation as possible responses depending on the rate of sea-level rise, the availability of sediment and the substrate.

The model used by Vousdoukas et al. (2020) is based on the combination of a background shoreline trend and Bruun's rule (Bruun, 1983). Bruun's rule is a contested method as both its accuracy (Ranasinghe et al., 2012) and validity (Anthony & Aagaard, 2020) have been questioned. The formula for Bruun's rule is:

$$s = la/h \quad (1)$$

With s ($m/year$) representing the movement of the depth of closure or shoreline, l (m) the length of the active profile, h (m) the height of the active profile and a ($m/year$) the rate of sea-level rise.

Other models like the one from Lorenzo-Trueba & Ashton (2013) have shown that adding the possibility of an additional sediment supply to a cross-shore profile can completely change its response to sea-level rise.

In this study the Holland coast will be taken as a case-study to obtain further insight in the response to sea-level rise.

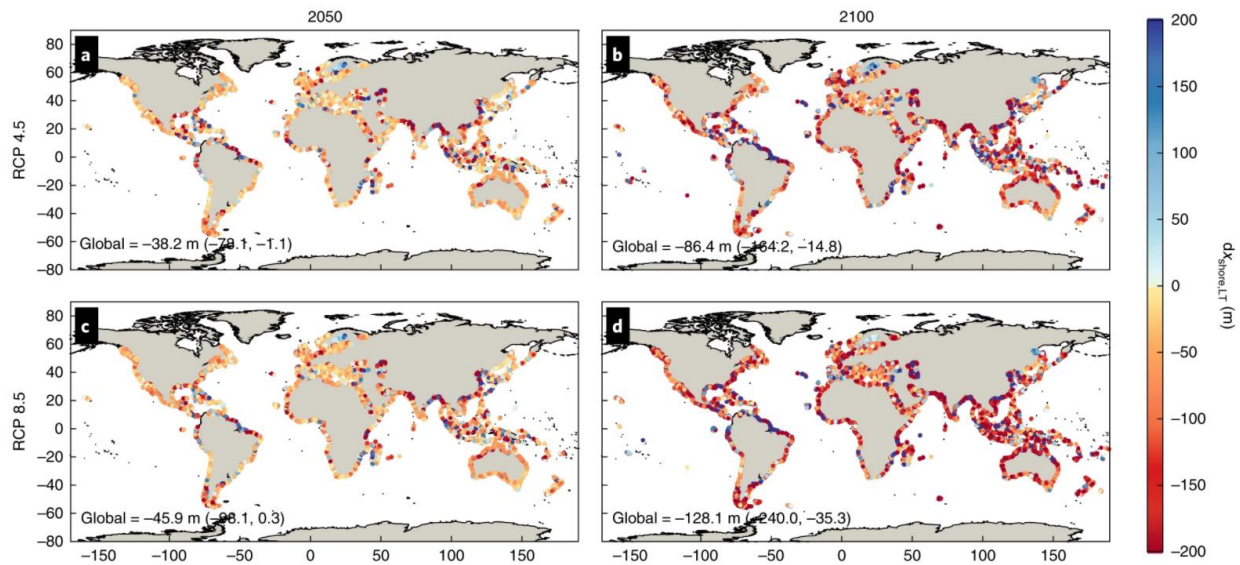


Figure 1 Projected shoreline changes in 2050 (a, c) and 2100 (b, d) for RCP 4.5 (top) and RCP 8.5 (bottom). Change is given as median relative to 2010. (Vousdoukas et al., 2020)

3.2 History of the Holland coast

The first known human seawalls along the coast date back to the 16th century (Wijnberg, 2002). It is known that in those times sections of the coast were eroding at a rate of 3-5 m/year, with groins being installed after 1800 to limit that erosion to 0.5-1.5 m/year (van Rijn, 2011). A yearly monitoring program (JARKUS) has been in place since 1963. Between 1964 and 1990 long term trends could not be found for the coast as a whole, but that different areas had different responses, with boundaries between areas often being found at locations where human intervention has taken place (Wijnberg & Terwindt, 1995). These boundaries are indicated in the figure below (Figure 2). Figures 3 & 4 show the results of the eigenfunction analysis done by Wijnberg & Terwindt (1995), illustrating the differences between the areas. For example, the different number of bars between the southern most part and the part just north of it. Since 1990 the main Dutch coastal policy is to maintain a set basal coastline using sand nourishments (Mulder et al., 2011). With a few exceptions for large scale projects, these nourishments are just noise when looking at timescales of decades or longer (Wijnberg, 2002). With the Pleistocene morphology still being relevant as well as a sediment source (Beets & van der Spek, 2000), a complicated picture is created. Making future predictions either using models or trends in historic data very difficult.

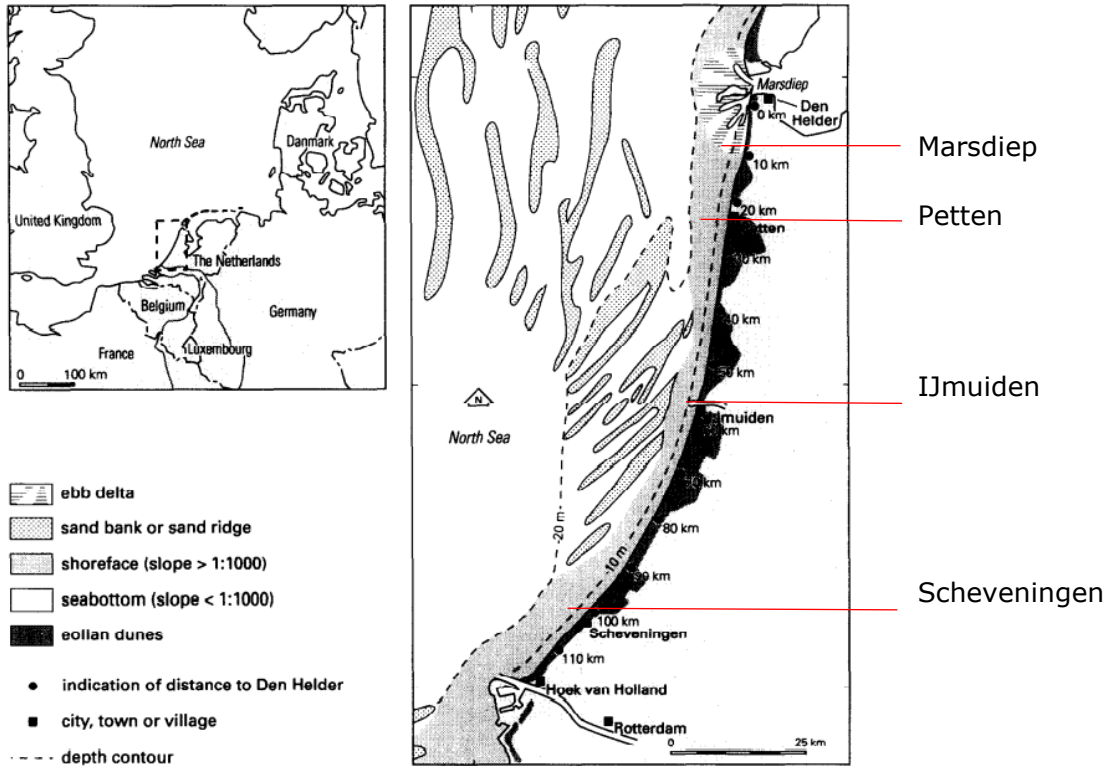


Figure 2 Overview of the Holland coast with locations of interest indicated. (Wijnberg & Terwindt, 1995)

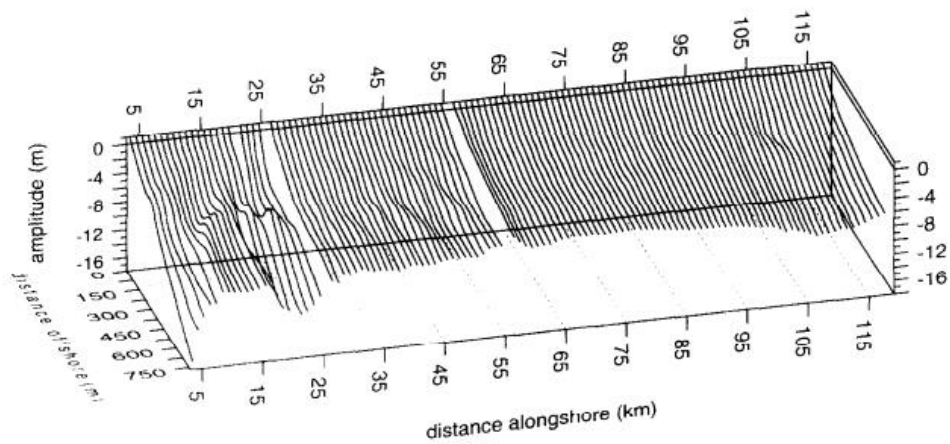


Figure 3 Time-averaged profiles along the Holland coast, as the first eigenfunction (Wijnberg & Terwindt, 1995)

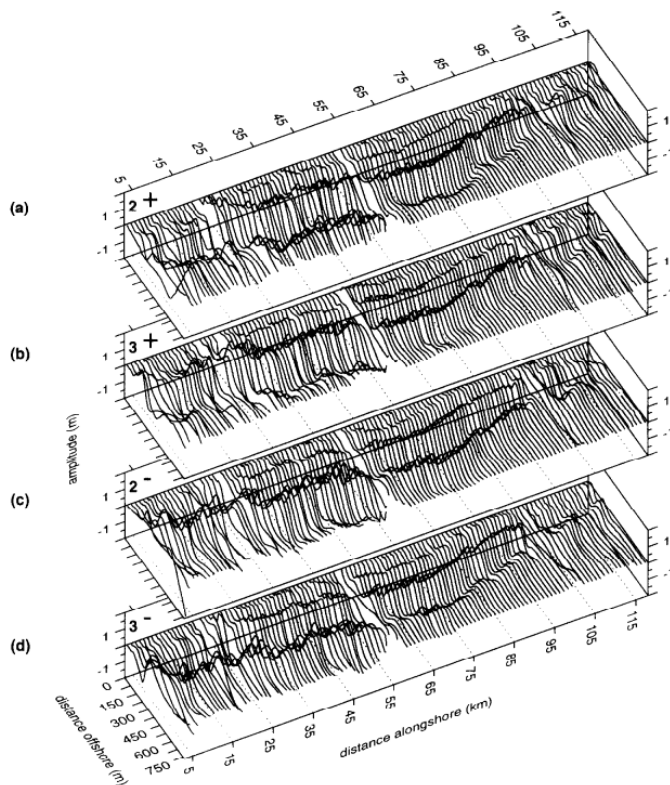


Figure 4 Secondary morphologies along the Holland coast. a) Second eigenfunction positively weighted, b) third eigenfunction positively weighted, c) second eigenfunction negatively weighted, d) third eigenfunction negatively weighted. (Wijnberg & Terwindt, 1995)

3.3 Holland coast response to sea-level rise

Various attempts at using the data from the Dutch coast to find trends and create closed sediment balances have been made. As mentioned above Wijnberg & Terwindt (1995) did not find a trend that could summarize the evolution of the whole coast at once, trends could only be found when the coast was split up into smaller sections. More recently, sediment balances for the Holland coast have shown that the system experiences losses under natural conditions, with the losses currently being offset by nourishments (De Ronde, 2008; van Rijn, 2011). To grow with a sea-level rise of 2 mm van Rijn (2011) found that a sediment volume of $0.4 \times 10^6 \text{ m}^3/\text{year}$ would be needed. Deltares (2018) estimated the volume needed to offset 2 mm sea-level rise at $8 \times 10^6 \text{ m}^3/\text{year}$. Currently this is covered by the nourishments, but accelerated sea-level rise would see this volume grow. The current nourishments are $12 \times 10^6 \text{ m}^3/\text{year}$, mainly placed between the depth contours of -5 and -8 (Deltares, 2018). This is also what Haasnoot et al. (2018) observe, with the addition that sea-level rise leads to more high-water events, thus less time for the coast to recuperate after an event leading to the sediment ending up in the more seaward part of cross-shore profiles. With one of the loss terms being alongshore transport, this would further strengthen the landwards movement of the shoreline already initiated with sea-level rise.

3.4 Modelled sea-level rise

As stated in section 3.1, it is assumed that the natural response of a coast to sea-level rise is that erosion will occur at the lower parts of the profile with deposition occurring at the beach, however there is a disconnect between the gradual, long time scale at which this occurs and the short, episodic erosion events (Masselink et al., 2020). Generally, models will therefore use a variation of the Bruun Rule, which uses equilibrium profiles and results in the expected landward and upwards shoreline response to sea-level rise.

However, use of this rule is contested as its strict assumptions mean that the quantitative accuracy of the rule is low (Ranasinghe et al., 2012). Furthermore, geography may be the control of the offshore boundaries, invalidating it further (Cowell & Kinsella, 2018). Instantaneous sea-level rise would result in oversteepening, due to differences between the decrease of onshore (faster) and offshore (slower) fluxes. Exact calculations of those fluxes, however, depend on whether they were calculated using linear wave theory or shallow water equations, as the difference between the values obtained with these two approaches increases with depth to possibly an order of magnitude (Ortiz & Ashton, 2016). Figure 5 illustrates these results, showing the cross-shore sediment transport based on the two methods.

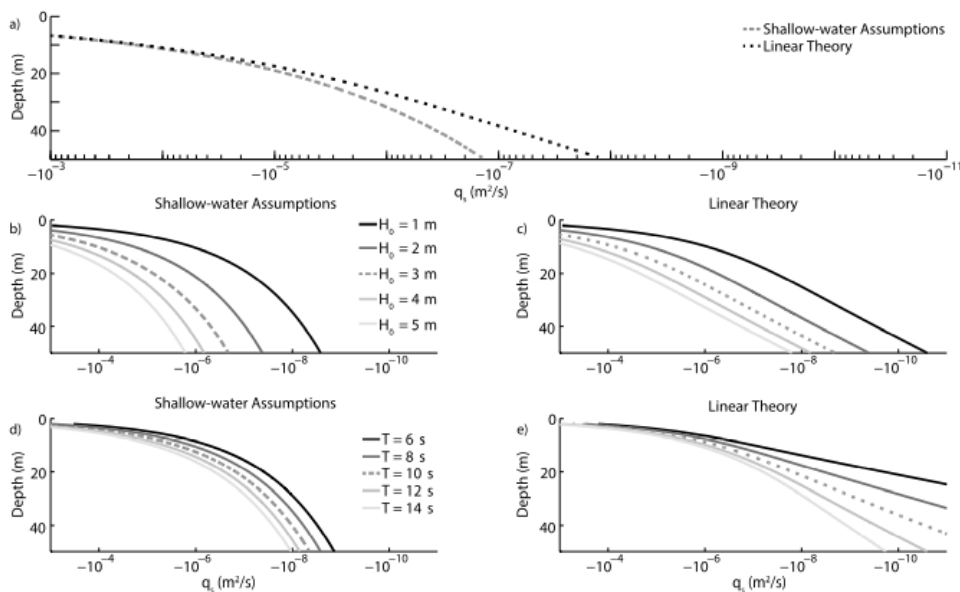


Figure 5 Sediment transport based on Shallow-water assumptions (left) and Linear theory (right). a) show a comparison of the approaches for $H_s=3\text{m}$ and $T=10\text{s}$. For b & c wave heights vary, for d & e wave periods vary. (Ortiz & Ashton, 2016)

These observations from data and modeling studies already show that there are timescale issues when looking at coastal response to sea-level rise. But there is one more significant issue when considering different works in literature; the offshore boundary used. This issue was clearly shown by Anthony & Aagaard (2020) who found several definitions for the term depth of closure. It has also been shown that this boundary is dependent on timescale (Lorenzo-Trueba & Ashton, 2013).

3.5 Depth of closure

Depth of Closure is a widely used term in coastal science, but what is meant with the term is inconsistent. A good overview of this problem is given in Anthony & Aagaard (2020). Generally, the depth of closure is defined as the seaward limit of the area with significant morphological change on a certain timescale. This is also the definition that will be used in this study, the depth of closure is at the depth where there is little morphological change on a decadal timescale. However, the depth of closure can be influenced by many factors like inherited topography (Kinsella et al., 2020) or tidal currents (Valiente et al., 2019). Figure 6 shows the processes that occur on and around the shoreface and gives an indication of where the depth of closure is with respect to the surrounding processes. Processes like undertow and longshore transport move sediment, thus result in significant morphological change, and occur above the depth of closure. Up- and downwelling on the other hand might stir some sediment but does not transport

it resulting in the depth of closure being defined above it. This figure is true for the depth of closure for short timescales, with increasing observation timescales the depth of closure will move deeper and further offshore (Udo et al., 2020).

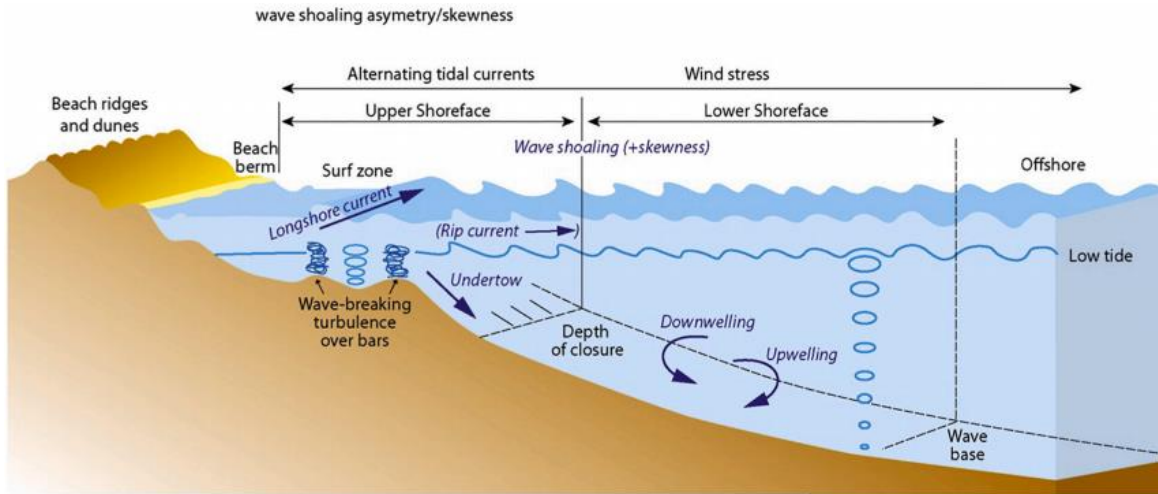


Figure 6 Diagram representing the main influences on the shoreface. (Anthony & Aagaard, 2020)

Commonly used formulas for estimating the depth of closure are based on significant wave height and associated wave period (Equations 2,3 & 4). These formulas were developed by Hallermeier (1978), Birkemeier (1985) and Capobianco et al. (1997). These formulas all contain significant wave height H_s (m), other used variables are the associated wave period T (s), the gravity acceleration constant $g = 9.81$ (m/s^2) and the constant K (-) which can be 3.4, 2.8 or 2.1 depending on the vertical variation in the profile. The formula proposed by Hallermeier (1978) is:

$$DoC = 2.28H_s - 68.5 \left(\frac{H_s^2}{gT^2} \right) \quad (2)$$

Birkemeier (1985) found that this over-predicted the depth of closure and adjusted the expression to:

$$DoC = 1.75H_s - 57.9 \left(\frac{H_s^2}{gT^2} \right) \quad (3)$$

Capobianco et al. (1997) proposed a simplified expression:

$$DoC = KH_s^{0.67} \quad (4)$$

This already shows that the result will vary greatly depending on the type of wave data used in the formula. If extreme values are given as input, the resulting depth of closure will correspond to that extreme scenario and be at a larger depth than if data for annually occurring storms are put in. For annually occurring storms at the Dutch coast wave heights and periods are in the order of 6 meters high with a period of 8 seconds (Li et al., 2014), resulting in depths of closure that, depending on the formula, vary between 6 and 12 meters. If the maximum values that the Dutch coastal protections are built to withstand are put in – wave height 9.5 meters and wave period 16.1 seconds (Ministerie van Verkeer en Waterstaat, 2007) – the depth of closure can vary between 10- and 20-meters depth. These and other examples of depths of closure for Dutch wave conditions are found in table 1.

Table 1 Depths of closure obtained with the different formulas using various wave data from the Holland coast.

Description	Hs (m)	T (s)	Depth of Closure from Hallermeier (1978) (m)	Depth of Closure from Birkemeier (1985) (m)	Depth of Closure from Capobianco (1997) with K=3.4 (m)	Depth of Closure from Capobianco (1997) with K=2.8 (m)	Depth of Closure from Capobianco (1997) with K=2.1 (m)
Storm 23 October 2002 (Aagaard et al., 2005)	3,8	6	5,9	4,3	8,3	6,8	5,1
Storm 26 October 2002 (Aagaard et al., 2005)	5	7	7,8	5,7	10,0	8,2	6,2
Storm 27 October 2002, 4th largest in period 1980- 2002 (Aagaard et al., 2005)	7,7	9	12,4	9,2	13,3	11,0	8,2
Yearly returning (Li et al., 2014)	6	8	9,8	7,2	11,3	9,3	7,0
Safety norm for Noord-Holland (Ministerie van Verkeer en Waterstaat, 2007)	9,5	16,1	19,2	14,6	15,4	12,7	9,5
Safety norm for Zuid-Holland (Ministerie van Verkeer en Waterstaat, 2007)	8,35	13,9	16,5	12,5	14,1	11,6	8,7

3.6 Shoreface response rate

Depth of closure is a boundary for the shoreface system and its evolution over time can be used to look at coastal response. However, a more direct way to look at coastal responses is to use the shoreface response rate. A large response rate means that the shoreface has a large ability of keeping its equilibrium shape during periods of sea-level change (Lorenzo-Trueba & Ashton, 2013).

These shoreface response rates were identified by Cowell & Kinsella (2018) as one of the critical knowledge gaps in predicting coastal responses to future sea-level rise. Especially when predicting for human lifetimes and management strategies.

A formula from Nienhuis & Lorenzo-Trueba (2019) can give an estimate for the shoreface response rate expected from wave data. This formula expresses the shoreface response rate ksf ($m^3m^{-1}year^{-1}$) as an equation of:

$$ksf = (3600 * 24 * 365) \frac{e_s c_s g^{\frac{11}{4}} H_s^5 T^2 \frac{1}{z_0} \frac{1}{z_0^{-D_T}}}{960 R \pi^2 \omega_s^2} \quad (5)$$

$$z_0 = \frac{H_s}{\gamma} \quad (6)$$

$$D_T = 0.018 H_s T \sqrt{\frac{g}{R D_{50}}} \quad (7)$$

$$\omega_s = \frac{R g D_{50}^2}{18 * 10^{-6} + \sqrt{\frac{3}{4} R g D_{50}^3}} \quad (8)$$

With equations 6,7 & 8 giving variables needed in equation 5. Constants used are the suspended sediment transport efficiency factor $e_s = 0.01$ (-), the friction factor $c_s = 0.01$ (-), the median grain size $D_{50} = 1 * 10^{-4}$ (m), wave breaking criterion $\gamma = 0.4$ (-) and the submerged specific gravity of sediment $R = 1.65$ (-).

3.8 Research question

The knowledge gaps that will be addressed in this study are the depth of closure and shoreface response rate based on historical profiles. For both these values there are many theories found in literature but there is very little to be found where they are obtained from bathymetry profiles. Especially profile measurements over a timescale longer than a few years. For the Dutch coast such a dataset is available and it will be used in this study to answer the following research question: How does sea-level rise affect the sediment balance on the shoreface of the Holland coast? To answer this question three sub-questions are considered. The first question is very basic: What is the depth of closure of the Holland coast? The second question is: What trends can be found in the depth of closure over time? And the last sub-question is: What is the shoreface response rate of the Holland coast? The results obtained from these questions will then be compared to results found in literature to obtain an answer to the main research question.

4. Methods

4.1 JARKUS data

The main dataset used for analysis is the JARKUS dataset (available from publicwiki.deltares.nl). It consists of yearly measurements of the bathymetry of the Dutch coast starting from 1964. Profiles are measured every 250 meters alongshore from the foredune to approximately 1-kilometer seawards, at which depths tend to be between -5 and -7 meters above NAP.

The JARKUS profiles are not consistent in the spacing between cross-shore measurement locations. This will be illustrated using the profile from 2020 at a location on the northern edge of Scheveningen (52.1195 latitude 4.2891 longitude). The inconsistency in the measurements is shown in figure 7a, on the seawards side of the profile there is a sequence with alternating values and missing values. Any missing values within the profiles were filled in using linear interpolation. The result of this interpolation is shown in figure 7b, However, there is still an issue that not all profiles are of the same length. Further analysis on the standard deviation is done using this stage, as the unequal length is dealt with in a later stage. For calculations using volumes the profiles were also extended seawards using a linear trend through all values below sea-level. These

extensions were set to not go below -20 depth to represent the situation of the North Sea best. The extrapolation itself can be seen in figure 7c, when the data was used only the parts that were not in the interpolated data were given the value of the extrapolation. This is only relevant for the seaward side of the profile.

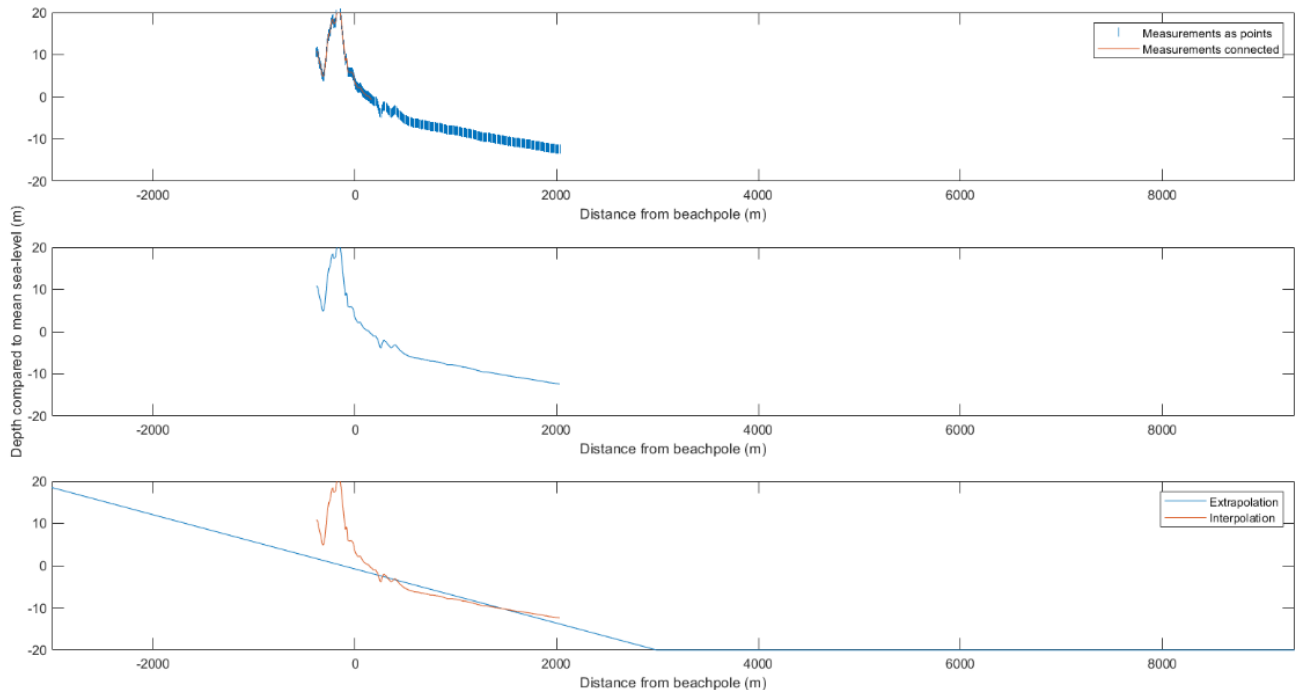


Figure 7 a) the raw altitude data, b) the linearly interpolated data, c) the linear extrapolation. All profiles are measured in 2020, at the location near Scheveningen 98.75 km south of Den Helder (JARKUS index 1393).

From this dataset a selection of profiles along the Holland coast was made. The Holland coast from Den Helder to Hoek van Holland contains 604 profiles. These profiles were tested through a series of requirements. They had to contain profiles for all 56 years, which left 357 profiles. Areas with large manmade or natural changes got excluded. In the northern most part this meant that profiles were only usable when the Marsdiep tidal channel no longer influences them, and in the south the boundary was the northern edge of the Scheveningen boardwalk. In between there are two areas excluded, the Hondsbossche en Pettemer seawall and the IJmuiden harbor jetties. With these exclusions 237 profiles remained. 40 were excluded in the north, 28 because of the seawall and 52 in the south. The profiles near IJmuiden had already gotten excluded due to a lack of profiles for all years. These boundaries are also the ones found by Wijnberg & Terwindt (1995) as boundaries for the blocks of homogeneous response along the Holland coast, and are shown in figure 2 (section 3.2). The selected profiles and the profile used for illustration are indicated in figure 8. It shows the beach poles for all JARKUS profiles, which results in a view of the coastline of The Netherlands and the beach poles belonging to the selected profiles. The profile that is used to illustrate processes with a single profile is marked with a yellow star.

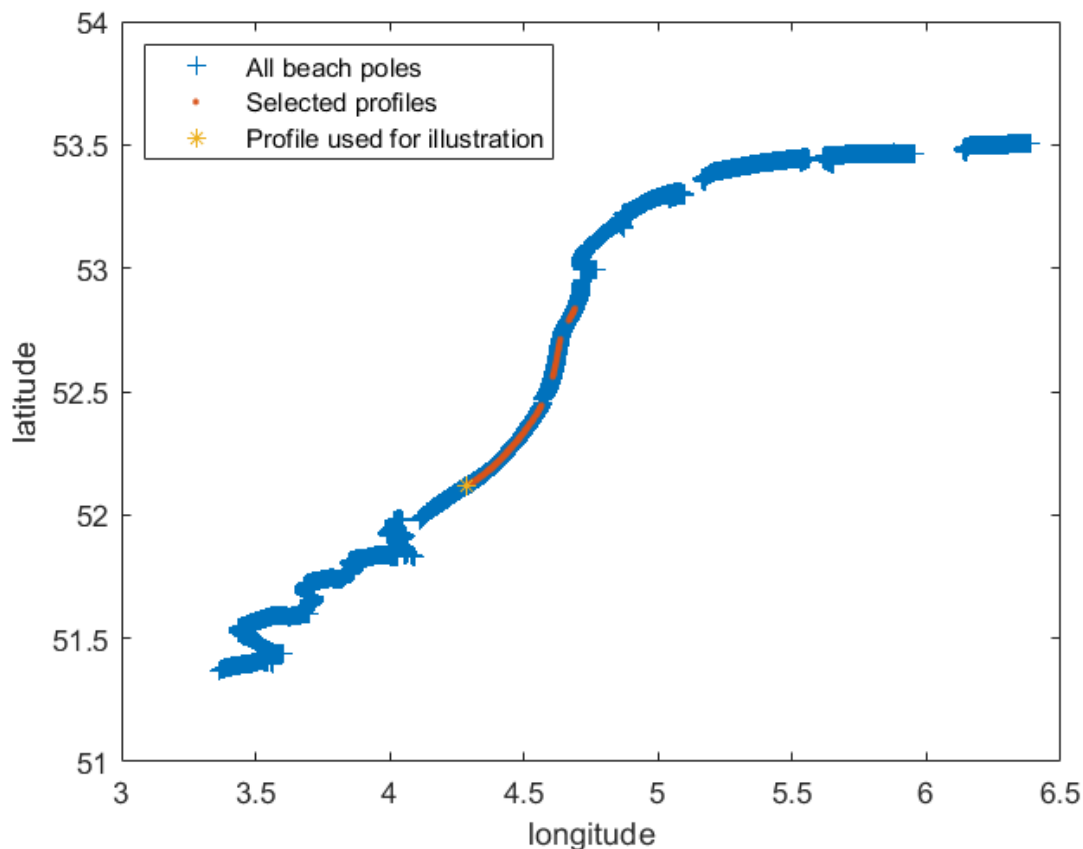


Figure 8 The profiles used in this study. Blue shows all beach poles along the Dutch coastline, orange the selected profiles and yellow the single profile used for illustration at 98.75 km south of Den Helder.

4.2 Depth of closure

To determine the depth of closure the standard deviation was used. This was done in two ways to determine the spatial and temporal variability, respectively. The first was to take all the available years at the same time and the second moving a fifteen-year time window over the years. The time window was moved using a forward-looking method. The standard deviation for timestep 1 is taken over the first fifteen years, timestep 2 over the years 2-16, until the point is reached where the last taken value for the window is the last one. After that, the size of the window became smaller with each next step, with the final timestep being the second to last one, taking the standard deviation over the last two years. For both methods, an exponential curve was fitted through the data to remove the sudden changes in standard deviation that occur due to profiles of different years not being the same length. This exponential was fitted from the maximum value of standard deviation until the seaward boundary of the cross-shore locations. The maximum of the standard deviation occurred at the peak of the dunes. From the standard deviation the depth of closure was determined by taking the first location below sea-level where the standard deviation drops below 0.1.

The spatial variability of the depth of closure values is then compared to the values that resulted from the wave-based formulas.

With the moving window this gives the changes in depth of closure over time. These depths of closure over time were then analyzed for possible trends. First each profile individually, by fitting a linear trend and looking whether that trend was positive (onshore directed) or negative (offshore directed). Secondly, all the profiles were taken

together and grouped in 5-year bins. This way an overall trend over time could be established and compared to the spatial variability over time.

4.3 Shoreface response rates

The secondary part of the analysis was to determine a shoreface response rate from the JARKUS data. There is no clear method or even a standard unit for shoreface response rate within literature. Here the same unit as the formulas from Nienhuis & Lorenzo-Trueba (2019) is used to allow comparison. In their model, which is based on that of Ortiz & Ashton (2016), they state that a shoreface response rate can be expressed as the integrated cross-shore sediment transport of a the active shoreface of a profile. To correspond with that, the choice was made to look at the yearly difference in a single profile between mean sea level and the depth of closure. To do this the extrapolated profiles are used as the profiles need to be of the same length. If it is assumed that the volume on a profile remains constant over time, the difference between profiles of following years will show the rate of sediment movement. For the profiles of the different years the difference was established by using a trapezoidal method to calculate the area between mean sea level and the profile for each profile, and then subtracting those two areas to obtain the difference.

5. Results

In the next sections of the results the spatial and temporal variability in the depth of closure of the Holland coast will be discussed and the shoreface response rate obtained. First, figure 9 illustrates how a profile evolves over time. The last year of this profile is the one used in the method section for illustration. All further results for a single profile also refer to this specific profile. The depth of closure for this profile is at -9.6 m, taking into account all the available years.

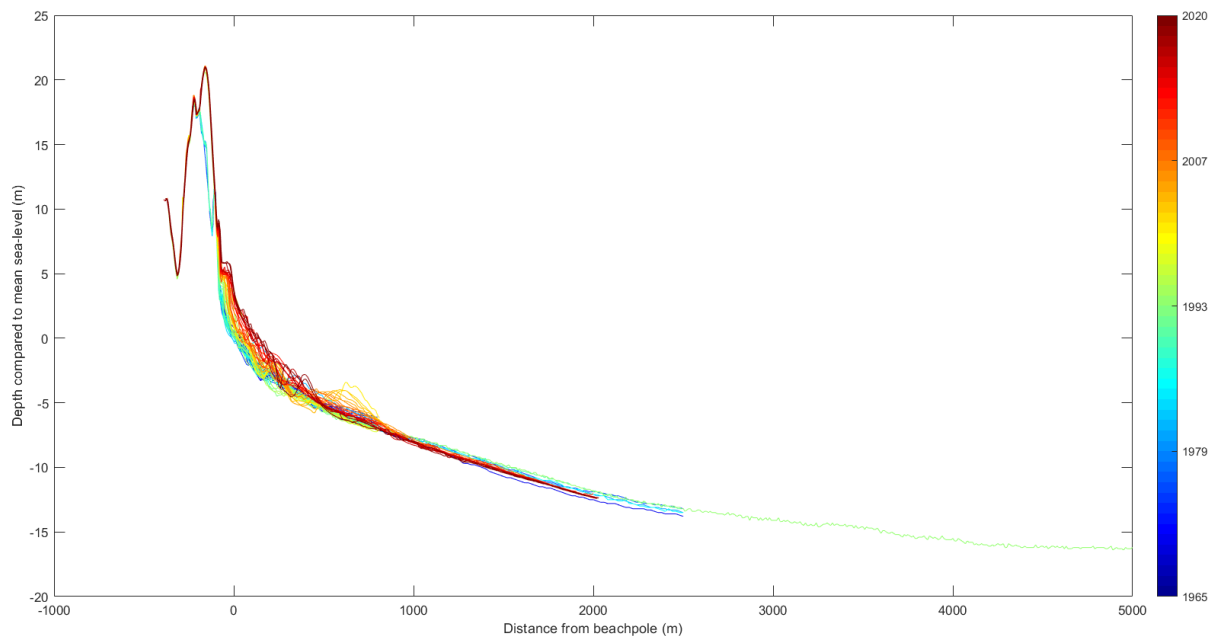


Figure 9 Profiles for every year from 1965 until 2020 at the selected profile 98.75 km south of Den Helder.

5.1 Depth of closure

Using the method that takes all the available years into account gives a single depth of closure for each profile. These depths of closure can vary greatly alongshore, as

illustrated by figure 10. The sections in the north between the Marsdiep & Petten and Petten & IJmuiden are relatively homogeneous within the section, but there is a large difference between the two sections. The section in the south between IJmuiden & Scheveningen shows a very large variability, with the largest depth of closure being located 70 km south of Den Helder. The smallest depth of closure also occurs within this section at approximately 82 km south of Den Helder.

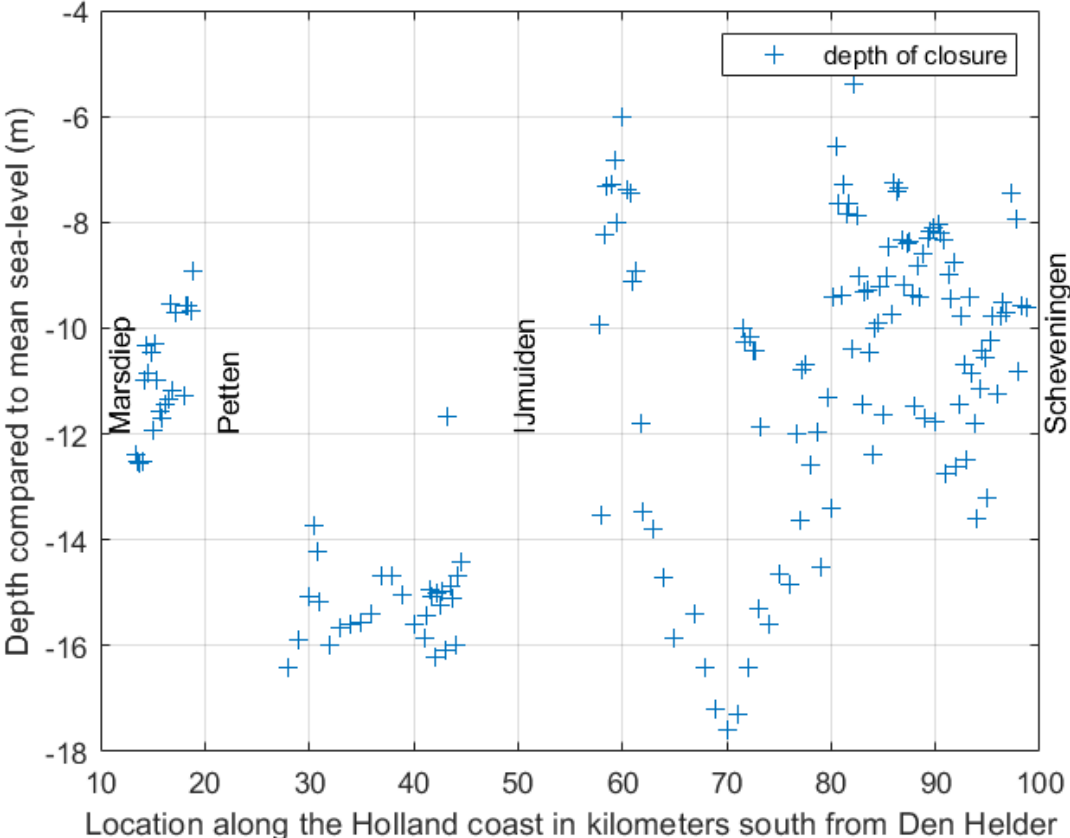


Figure 10 Depth of closure for each profile along the Holland coast.

5.2 Depth of closure trends

For the temporal variability in depth of closure the quantity of the results becomes much larger, as there is a depth of closure for each timestep for every profile. To start simple the depth of closure for each timestep of the selected profile is shown in figure 11. This figure also contains a linear trend fitted through the data with its confidence interval. The depth of closure for this profile has changed a lot over the years. There is a period where it moved onshore, between 1976 and 1982, after which it moved offshore until 1990. From 1998 until 2019 there is a clear movement onshore. Overall, this has resulted in a positive linear trend, showing that the depth of closure is moving onshore over time.

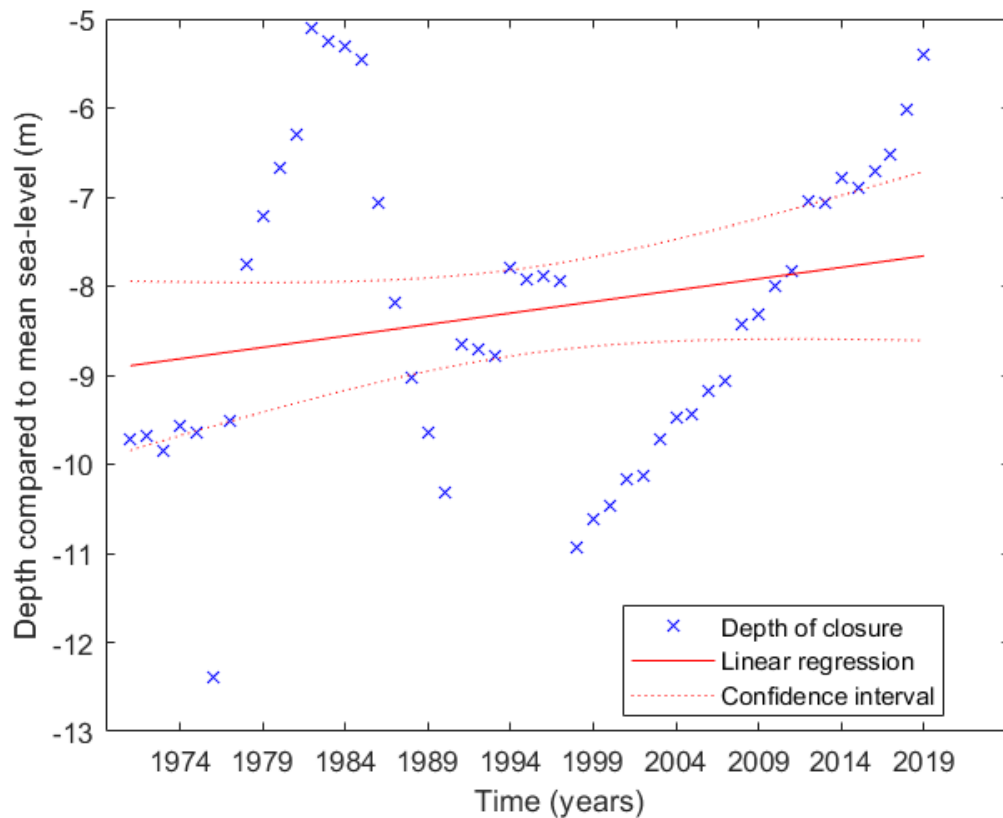


Figure 11 Temporal variability in the depth of closure for the selected profile. A linear trend is fitted through with the 95% confidence interval.

However, taking those trends for every profile again shows the large longshore variability. Figure 12 shows the slope coefficient for the linear trend of every profile. As in Figure 11, a positive coefficient means that the depth of closure is moving onshore and a negative offshore. Without looking at each profile individually it is impossible to see any indications of an overall trend. Instead, a range of positive and negative trends are found along the coast.

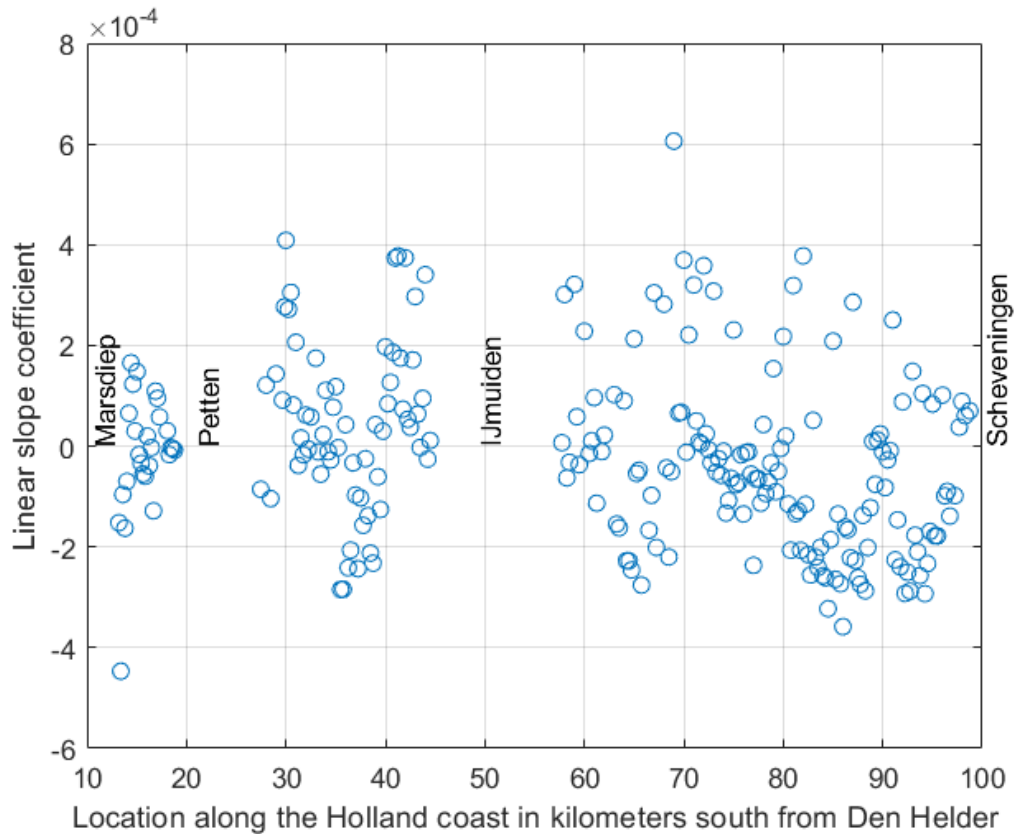


Figure 12 Linear slope coefficient for the model fitted through the depth of closure over time. A positive slope coefficient means that the depth of closure moves onshore, a negative offshore.

Aggregating all the profiles to look for a trend that could be related to sea-level rise gives the following results. Figure 13 shows a boxplot of the depths of closure for all profiles binned in five-year time intervals. This again shows that there is a large variability in longshore depths of closure, larger than the variability over time. Figure 14 shows a linear trend plotted through the mean of each of the bins. The large confidence interval shows that the trend is very unclear and could still change direction within the confidence interval. This implies that there is no trend in depth of closure recognizable for the Holland coast as a whole.

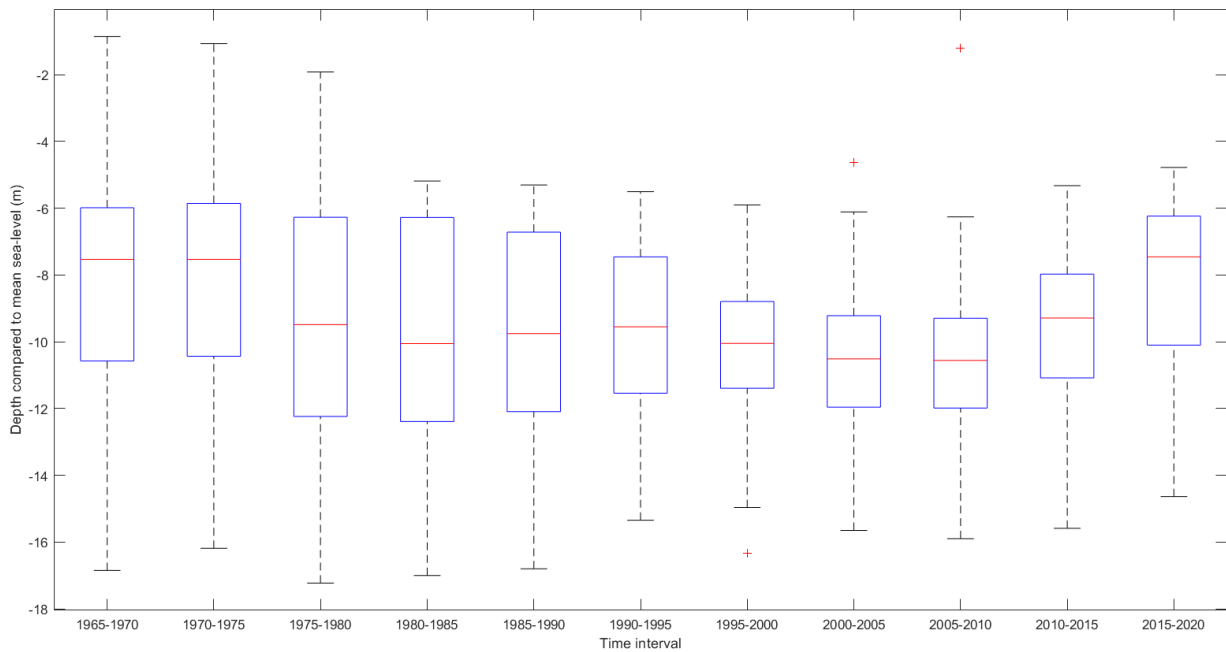


Figure 13 Boxplot of the 5-year bins with all profiles aggregated.

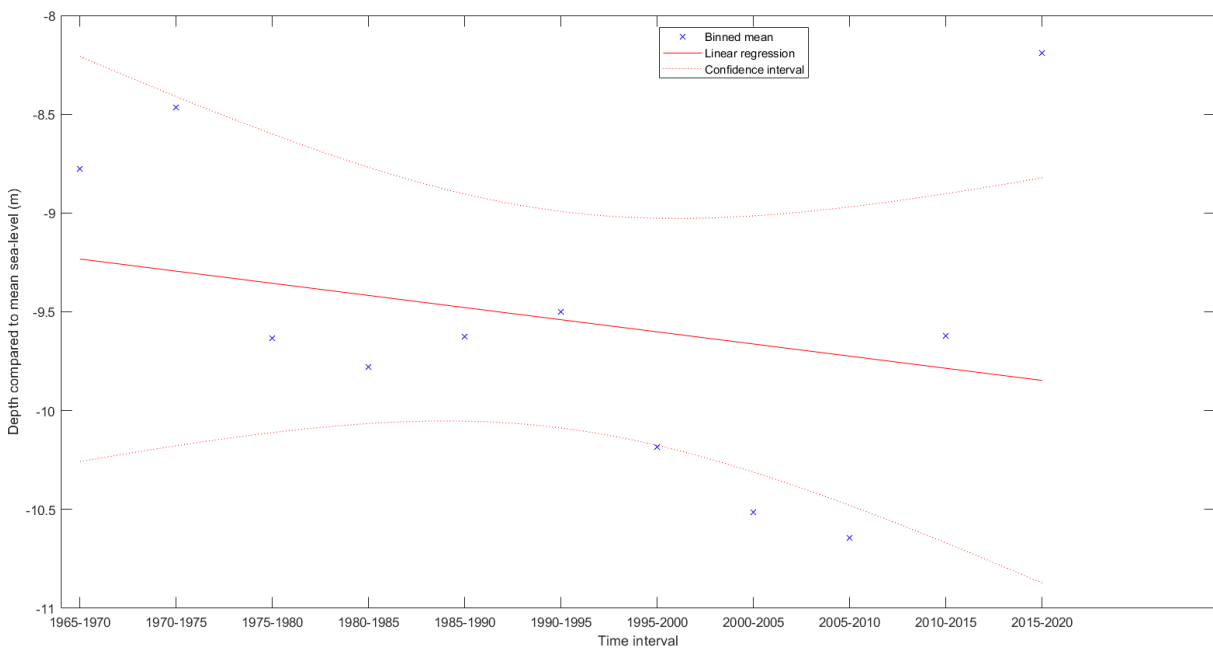


Figure 14 Linear trend fitted through the means of the 5-year bins, with the 95% confidence interval.

5.3 Shoreface response rate

The final part of the analysis of the JARKUS data was done to obtain shoreface response rates. The order of magnitude obtained by taking the difference between following years is between $1 \cdot 10^3 \text{ m}^3\text{m}^{-1}\text{year}^{-1}$ and $1 \cdot 10^4 \text{ m}^3\text{m}^{-1}\text{year}^{-1}$ depending on profile and year. In comparison the formula of Nienhuis & Lorenzo-Trueba (2019) (Equation 5) which is based on wave climate gives an order of magnitude of $1 \cdot 10^5 \text{ m}^3\text{m}^{-1}\text{year}^{-1}$, when used with a wave height of 6 meters and a wave period of 8 seconds, the values for annually returning storms (Li et al., 2014).

6. Discussion

6.1 Spatial variability

There is an easy explanation for the alongshore variability, as the location of the largest depth of closure corresponds with a known location of tidal sand waves. At the location, which is near Zandvoort, there are tidal sand waves at a depth between 14 and 18 meters (Van Dijk & Kleinhans, 2005). These tidal sand waves are morphodynamically active, thus resulting in them being included in an active zone when basing the boundaries on standard deviations. However, the dominant process in their development are the tidal currents and they are spread all over the North Sea, indicated as sand ridges in figure 2 (section 3.2). Therefore, they should not be included when looking at the depth of closure over decadal timescales for the Holland coast. The actual depth of closure for wind wave-based processes would be less deep, but cannot be found using this method.

Other variations are not as easily explained. Some may occur due to variations in the longshore transport of sediment. Especially around the harbor jetties of IJmuiden this transport gets disrupted. But another explanation can also be found in Dutch coastal policy. Since 1990, the main part of the policy consists of nourishments but there are also other coastal defense structures. All of which can lead to possibly extreme longshore variability (Van Rijn, 2011). It can be noted that the longshore variability has decreased with time, as shown in figure 13. The reason for this is unclear, it could be that this is a result of the management strategies, but it is also possible that it is an artefact of the evolution in measurement techniques for profiles.

Overall, the results show that a depth of closure of about 12 meters below sea-level would be a good approximation for the Holland coast on decadal timescales. The wave-based formulas used with a storm with a decadal return period (table 1) and the JARKUS data both seem to reach that value. However, they also reiterate the point Valiente et al. (2019) made, namely that there can be large variations in the results both because of estimation methods and because a lot of naturally occurring alongshore variability. Ortiz & Ashton (2016) confirm that using different methods may lead to very different depths of closure, and state that the timescale that is being considered in the study should influence the choice of method.

6.2 Time evolution

For a single profile, the trend in depth of closure over time is relatively easy to explain. Figure 9 shows a profile just north of Scheveningen where a nourishment was made in 1999. The nourishment was added seawards of the zone with sandbars, at a cross-shore distance between 600- and 700-meters seawards of the beach pole. Figure 11 shows the corresponding depth of closure values and their trend. Here it can be seen that the depth of closure suddenly moved further offshore when the nourishment was placed, starting from the year before the nourishment (1998) as a result of the forward-looking method used. Then, gradually the depth of closure moved landwards as the sand in the nourishment got distributed over the profile. This results in a trend of the depth of closure moving landwards. It is unclear if this is because it is pushed landwards by sea-level rise or if the nourishment pushed it further seawards and it is simply returning to its previous location.

As shown in the example of this selected profile, human interference, such as the placement of nourishments, can influence the trend in depth of closure of a single profile. With the widespread nourishing that occurs at the Holland coast it is therefore unsurprising that there is a large variability in the trends found for every profile separate and that there is no clear trend when aggregating all profiles. This also means that the current sea-level rise does not result in an overruling trend.

These results contrast with simple model predictions using Bruun's rule (Equation 1). Applying it with the 0.2 meters of sea-level rise the Dutch coast has experienced over the last century (De Ronde, 2008) and the slope calculated with the previous estimations for depth of closure shows that it is expected for the depth of closure to move onshore. This is also the expectation using the model by Lorenzo-Trueba & Ashton (2013) unless there is an additional sediment supply. Which is the case for the Holland coast, thus explains why the reality does not correspond with model predictions. The current nourishment policy overcompensates for both loss to different parts of the system and sea-level rise (van Rijn, 2011), which explains why depths of closure can also move offshore for areas of the Holland coast.

Another point made by Cowell & Kinsella (2018) that could also be in play is that there is a time lag between the change in sea-level rise and the adjustment of the shoreface, which is mostly relevant for the decadal to centennial timescales that are looked in this study. Masselink et al. (2020) further point out that there is a disconnect in the gradual changes in sea-level rise and the episodic occurrences of coastal erosion or the large movement of sediments that occur during storm events. These timescale issues are partly addressed by the large amount of data in the JARKUS dataset. But, with the measurements done only once a year, the difference between a storm or a calm season cannot be seen. Although, that is advantageous when searching for trends over decadal timescales.

6.3 Shoreface response rate

That the value found for the shoreface response rate from the JARKUS data is much lower than that found from the wave climate can likely be explained by transport alongshore. The assumption made for the analysis was that the total volume of sediment on a profile would remain constant between years, sediment would just move cross-shore. This means that any gradient in alongshore transport will violate that assumption, resulting in a seemingly smaller amount of total transport than has occurred in reality. Considering that van Rijn (2011) found a longshore loss of $0.3 \cdot 10^6 \text{ m}^3 \text{ year}^{-1}$ towards the Waddensea when looking at the sediment balance of the Dutch coast, it is very likely that this assumption is indeed violated. On the other hand, the value obtained from the formula using the wave climate uses the wave data for an annually returning storm, not the average wave conditions during a year, leading to a possible overestimation of the total sediment transport that would occur.

As mentioned before, there is very little about shoreface response rates to be found in literature. However, there have been several studies that have reported on the development of nourishments. Grunnet & Ruessink (2005) found that a nourishment of $450 \text{ m}^3 \text{ m}^{-1}$ in front of Terschelling caused a quick reaction to move the profile out of its regular state, this occurred within half a year. The return to the regular state occurred gradually, with normal bar migration patterns resuming after 6-7 years. They also note that the sediment from the nourishment moved in the longshore direction at a speed of 400 m/year. This furthers the point made above that a purely cross-shore view is incomplete when considering the shoreface response. However, Ojeda et al. (2008) found no alongshore migration of nourishments at Egmond and Noordwijk. They found a cross-shore migration rate at Noordwijk of 0.14 m/day or 51.1 m/year for a volume of $1,71 \cdot 10^6 \text{ m}^3$, spread over 3 km so about $570 \text{ m}^3 \text{ m}^{-1}$. This is again a movement speed of a volume, not a shoreface response rate by the definition used in this study. Huisman et al. (2019) do utilize the same unit as this study, but only look at the erosion rates of a nourishment. They found an average erosional rate of nourishments of $34 \text{ m}^3 \text{ m}^{-1} \text{ year}^{-1}$. Looking more geometrically they found a mean erosion rate of $32 \text{ m}^3 \text{ m}^{-1} \text{ year}^{-1}$ in the trough with an associated mean accretion in the nearshore at a rate of $46 \text{ m}^3 \text{ m}^{-1} \text{ year}^{-1}$. They found very little volume changes seawards of the nourishment. The nearshore accretion can

exceed the erosion rate at the nourishment, in those cases there must be an additional source which can either be the trough or a different region. Again showing that it is very limiting to look at a single profile.

The value for total shoreface response rate that is obtained by adding all observed volume changes from Huisman et al. (2019) is in the order of magnitude of $1 \cdot 10^2$, which is one to two orders of magnitude smaller than the values found in this study. Boundaries were set slightly different, but a possible source of the difference is the extrapolation method used in this study to extend the profiles. This method can lead to an over estimation of the changed volume if there is a difference in the steepness of the profiles.

All in all, the shoreface response rate remains a very uncertain parameter. Further verification of the shoreface response rates obtained from real profiles remains a necessity and could be crucial in understanding how coasts will respond to changing conditions. Trends in depth of closure can be used for analysis of coastal response, but in areas with significant human interventions in the system, they tell very little about the natural processes. Applying this method in areas with no human intervention should give more information on the natural response mechanisms of coasts, which could be the topic of a further study.

7. Conclusions

In this study the effects of sea-level rise on the Holland coast are investigated. The yearly bathymetry measurements are used to determine depths of closure and shoreface response rates. The depths of closure are then analyzed to find trends in behavior that could be related to sea-level rise.

The current depth of closure for the Holland coast varies greatly alongshore, with a mean value of approximately 12 meters below mean sea-level.

The variation of the depth of closure over time shows no clear pattern or trend. The variation between the profiles is larger than the variation over time. A closer look at a single profile shows that any trend in the depth of closure is greatly influenced when nourishments are placed on the profile. As current Dutch coastal safety policy mainly consists of nourishments, it is impossible to find any reflection of natural processes in the data from the Holland coast.

Shoreface response rates remain very poorly understood. Here differences between integrated profiles result in shoreface response rates between the orders of magnitude of $1 \cdot 10^3 - 1 \cdot 10^4 \text{ m}^3\text{m}^{-1}\text{year}^{-1}$. However, comparisons with other values found in previous studies show that other studies found different orders of magnitude. Further research in this will be necessary for understanding and predicting the future of coastal zones.

In the end this study shows that the Holland coast is currently controlled by human interferences in the system. If the nourishment strategy remains, this will continue to be the main influence on the shoreface. To look at the reaction of a shoreface to processes like sea-level rise more research would need to be done in areas that are not heavily influenced by humans.

8. References

- Aagaard, T., Kroon, A., Andersen, S., Sørensen, R. M., Quartel, S., & Vinther, N. (2005). Intertidal beach change during storm conditions; Egmond, The Netherlands. *Marine geology*, 218(1-4), 65-80.
- Anthony, E. J., & Aagaard, T. (2020). The lower shoreface: Morphodynamics and sediment connectivity with the upper shoreface and beach. *Earth-Science Reviews*, 103334.
- Beets, D. J., & van der Spek, A. J. (2000). The Holocene evolution of the barrier and the back-barrier basins of Belgium and the Netherlands as a function of late Weichselian morphology, relative sea-level rise and sediment supply. *Netherlands Journal of Geosciences*, 79(1), 3-16.
- Birkemeier, W. A. (1985). Field data on seaward limit of profile change. *Journal of Waterway, Port, Coastal, and Ocean Engineering*, 111(3), 598-602.
- Bruun, P. (1983). Review of conditions for uses of the Bruun rule of erosion. *Coastal Engineering*, 7(1), 77-89.
- Capobianco, M., Larson, M., Nicholls, R. J., & Kraus, N. C. (1997). Depth of closure: A contribution to the reconciliation of theory, practice, and evidence. In *Coastal Dynamics' 97* (pp. 506-515). ASCE.
- Cooper, J. A. G., Masselink, G., Coco, G., Short, A. D., Castelle, B., Rogers, K., ... & Jackson, D. W. T. (2020). Sandy beaches can survive sea-level rise. *Nature Climate Change*, 10(11), 993-995.
- Cowell, P. J., & Kinsela, M. A. (2018). Shoreface controls on barrier evolution and shoreline change. In *Barrier dynamics and response to changing climate* (pp. 243-275). Springer, Cham.
- De Ronde, J. G. (2008). Toekomstige langjarige suppletiebehoefte. *Deltares report Z*, 4582.
- Grunnet, N. M., & Ruessink, B. G. (2005). Morphodynamic response of nearshore bars to a shoreface nourishment. *Coastal Engineering*, 52(2), 119-137.
- Haasnoot, M., Bouwer, L., Diermanse, F., Kwadijk, J., Van der Spek, A., Essink, G. O., ... & Huismans, Y. (2018). *Mogelijke gevolgen van versnelde zeespiegelstijging voor het Deltaprogramma: een verkenning*. Deltares.
- Hallermeier, R. J. (1978). Uses for a calculated limit depth to beach erosion. In *Coastal Engineering 1978* (pp. 1493-1512).
- Huisman, B. J., Walstra, D. J. R., Radermacher, M., de Schipper, M. A., & Ruessink, B. G. (2019). Observations and modelling of shoreface nourishment behaviour. *Journal of Marine Science and Engineering*, 7(3), 59.
- Kinsela, M. A., Hanslow, D. J., Carvalho, R. C., Linklater, M., Ingleton, T. C., Morris, B. D., ... & Woodroffe, C. D. (2020). Mapping the Shoreface of Coastal Sediment Compartments to Improve Shoreline Change Forecasts in New South Wales, Australia. *Estuaries and coasts*, 1-27.
- Li, F., Van Gelder, P. H. A. J. M., Ranasinghe, R., Callaghan, D. P., & Jongejan, R. B. (2014). Probabilistic modelling of extreme storms along the Dutch coast. *Coastal Engineering*, 86, 1-13.
- Lorenzo-Trueba, J., & Ashton, A. D. (2014). Rollover, drowning, and discontinuous retreat: Distinct modes of barrier response to sea-level rise arising from a simple morphodynamic model. *Journal of Geophysical Research: Earth Surface*, 119(4), 779-801.
- Masselink, G., Russell, P., Rennie, A., Brooks, S., & Spencer, T. (2020). Impacts of climate change on coastal geomorphology and coastal erosion relevant to the coastal and marine environment around the UK. *MCCIP Science Review, 2020*, 158-189.
- Ministerie van Verkeer en Waterstaat (2007) *Hydraulische Randvoorwaarden 2006 voor het toetsen van primaire waterkeringen* (in Dutch). Technical Report; Ministerie van Verkeer en Waterstaat

- Mulder, J. P., Hommes, S., & Horstman, E. M. (2011). Implementation of coastal erosion management in the Netherlands. *Ocean & coastal management*, 54(12), 888-897.
- Nicholls, R. J., & Cazenave, A. (2010). Sea-level rise and its impact on coastal zones. *science*, 328(5985), 1517-1520.
- Nienhuis, J. H., & Lorenzo-Trueba, J. (2019). Simulating barrier island response to sea level rise with the barrier island and inlet environment (BRIE) model v1.0. *Geoscientific Model Development*, 12(9), 4013-4030.
- Ojeda, E., Ruessink, B. G., & Guillen, J. (2008). Morphodynamic response of a two-barred beach to a shoreface nourishment. *Coastal Engineering*, 55(12), 1185-1196.
- Ortiz, A. C., & Ashton, A. D. (2016). Exploring shoreface dynamics and a mechanistic explanation for a morphodynamic depth of closure. *Journal of Geophysical Research: Earth Surface*, 121(2), 442-464.
- Ranasinghe, R., Callaghan, D., & Stive, M. J. (2012). Estimating coastal recession due to sea level rise: beyond the Bruun rule. *Climatic Change*, 110(3-4), 561-574.
- Stive, M. J. (2004). How important is global warming for coastal erosion? *Climatic Change*, 64(1-2), 27.
- Udo, K., Ranasinghe, R., & Takeda, Y. (2020). An assessment of measured and computed depth of closure around Japan. *Scientific reports*, 10(1), 1-8.
- Van Dijk, T. A., & Kleinans, M. G. (2005). Processes controlling the dynamics of compound sand waves in the North Sea, Netherlands. *Journal of Geophysical Research: Earth Surface*, 110(F4).
- Van Rijn, L. C. (2011). Coastal erosion and control. *Ocean & Coastal Management*, 54(12), 867-887.
- Vousdoukas, M. I., Ranasinghe, R., Mentaschi, L., Plomaritis, T. A., Athanasiou, P., Luijendijk, A., & Feyen, L. (2020). Sandy coastlines under threat of erosion. *Nature climate change*, 10(3), 260-263.
- Wijnberg, K. M. (2002). Environmental controls on decadal morphologic behaviour of the Holland coast. *Marine Geology*, 189(3-4), 227-247.
- Wijnberg, K. M., & Terwindt, J. H. (1995). Extracting decadal morphological behaviour from high-resolution, long-term bathymetric surveys along the Holland coast using eigenfunction analysis. *Marine Geology*, 126(1-4), 301-330.

Webservices:

<https://publicwiki.deltares.nl/display/OET/Dataset+documentation+JarKus>